Expanded View Figures

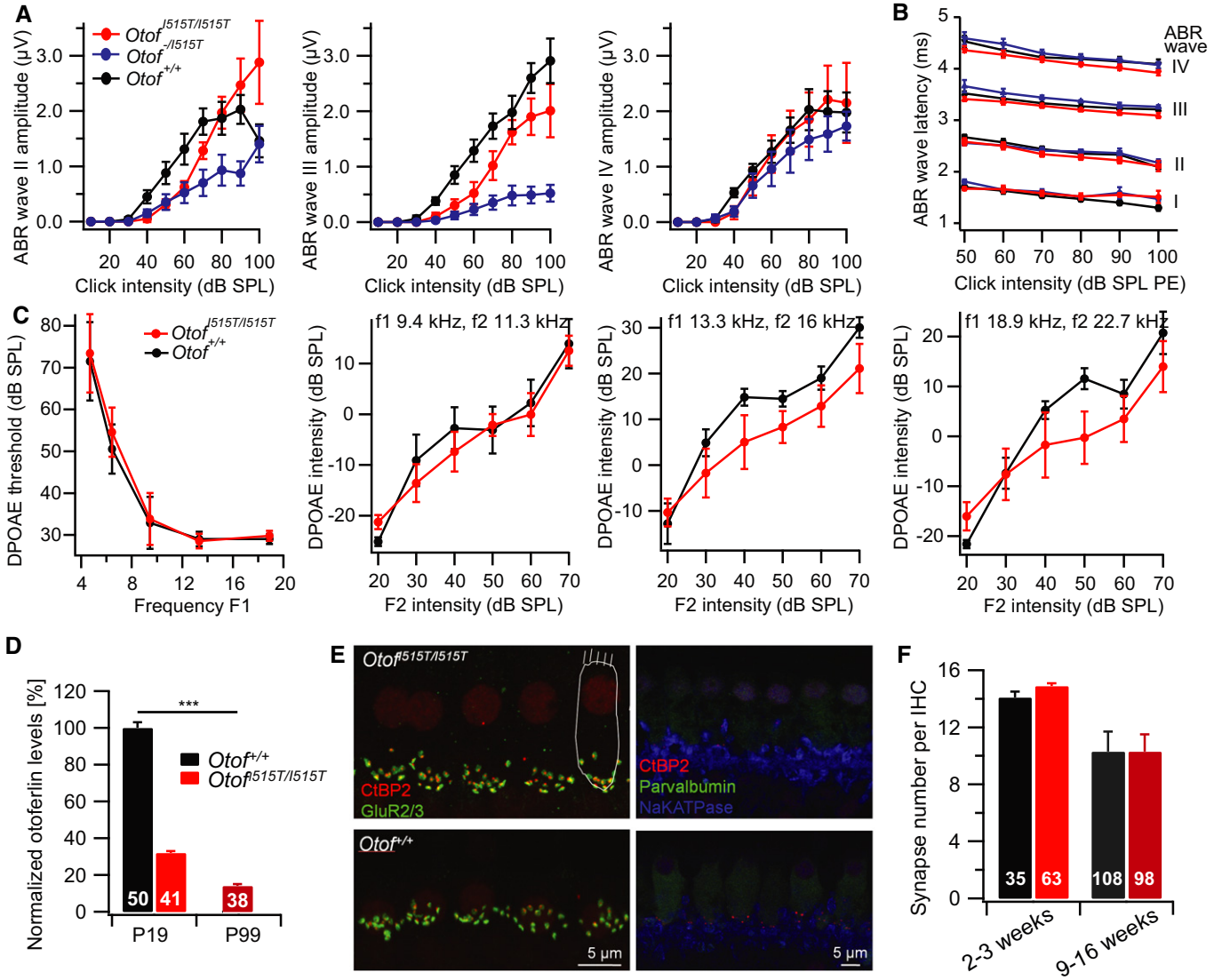

Figure EV1. Partial central compensation of ABR wave I amplitude reduction, otoferlin protein levels during ageing and intact cochlear amplification.

A Amplitude growth of ABR waves II-IV with rising stimulus intensity to click stimulation in *Otof*$^{I515T/I515T}$ (red, n = 5), *Otof*$^{-/I515T}$ (blue, n = 6) and *Otof*$^{+/+}$ (black, n = 5) animals tested at an age of 3–4 weeks, indicating a severe deficit of synchronous spiral ganglion neuron activation in *Otof* mutants but partial compensation in the auditory brainstem (mean ± SEM).

B Latencies of ABR waves I–IV from the same data set.

C Left: Interpolated DPOAE thresholds determined as the F1 intensity at which DPOAE intensity reached −10 dB SPL are comparable between *Otof*$^{I515T/I515T}$ (red) and *Otof*$^{+/+}$ (black) mice. Right: Amplitude growth of DPOAE in response to pairs of sine waves (frequencies indicated above each panel) at rising intensities. F1 intensity was always 10 dB above F2 intensity.

D Otoferlin protein levels were even further reduced during ageing in *Otof*$^{I515T/I515T}$ IHCs, explaining the age-dependent decrease in ABR amplitudes. Numbers indicate number of IHCs analysed (Tukey–Newman–Keuls test for parametric multiple comparisons; ***$P < 0.001$).

E Representative images used for synapse counting in *Otof*$^{I515T/I515T}$ (top) and *Otof*$^{+/+}$ (bottom) IHCs. For 2- to 3-week-old mice (left), z-projections of confocal stacks stained for ribbons (CtBP2, red) and postsynaptic glutamate receptors (GluR2/3, green) are shown. For 9- to 16-week-old mice (right), single sections of IHCs imaged in z-stacks, stained for ribbons (CtBP2, red), the cytoplasmatic calcium buffer parvalbumin (green) and SGNs stained for Na/K-ATPase (blue) are shown.

F Quantification of synapses; numbers indicate the number of IHCs analysed; mean ± SEM.

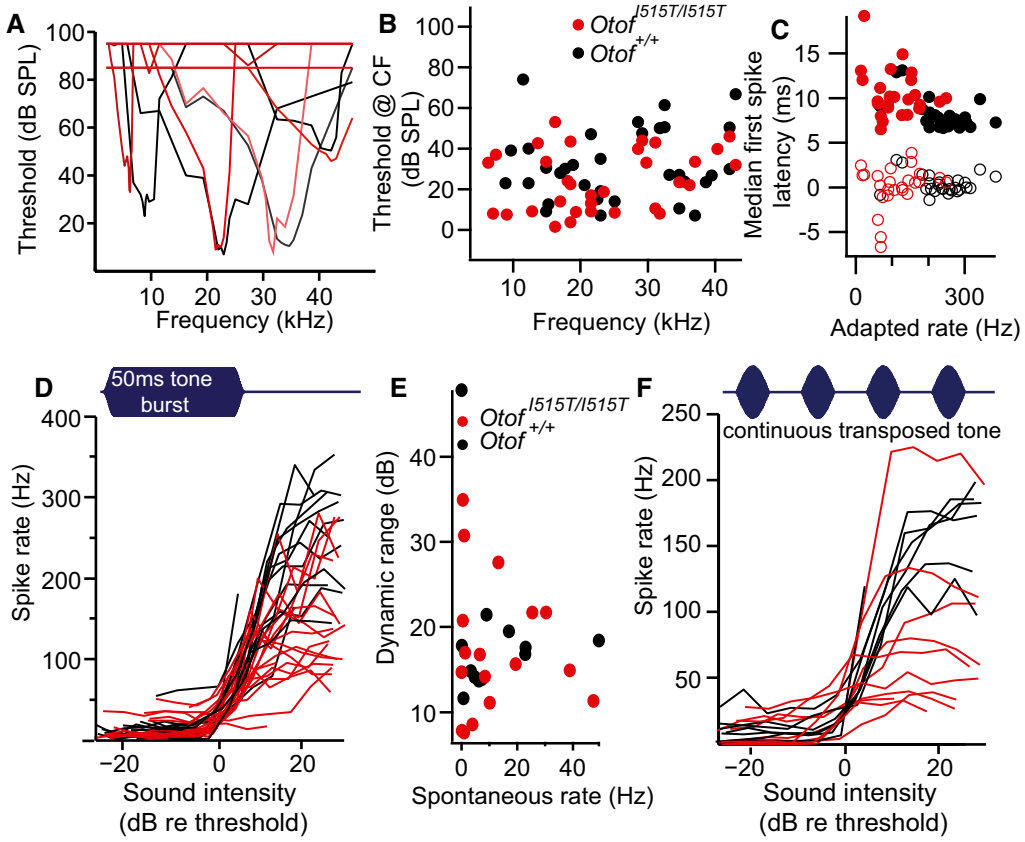

Figure EV2. Single SGN responses show normal frequency tuning and thresholds, but abnormalities of latencies and spike rates.

A Representative examples of SGN tuning curves from *Otof*$^{I515T/I515T}$ (pink/red) and *Otof*$^{+/+}$ (grey/black) mice.

B Thresholds at CF were comparable in *Otof*$^{I515T/I515T}$ (red) and *Otof*$^{+/+}$ (black) SGNs.

C The median first spike latency (FSL) in response to 200 repetitions of tone bursts at CF, 30 dB above threshold at a stimulus rate of 5 Hz was significantly prolonged in *Otof*$^{I515T/I515T}$ (red closed circles) and *Otof*$^{+/+}$ (black closed circles) (P = 0.0003, t-test). However, when the expected median FSL for the respective onset spike rate was subtracted (open symbols), FSLs were normal. The expected median FSL was calculated by the following formula which was derived from a large population of wild-type SGNs: $-2.5 \times$ log(onset rate) + 20.23. All FSL estimates were first corrected for the system delay (3.6 ms), for the time of the 4 ms tone burst ramp to reach fibre threshold and for the travelling wave delay (up to 0.8 ms according to our wild-type data set).

D Spike rate increases in individual *Otof*$^{I515T/I515T}$ (red) SGNs in response to tone burst stimulation at CF and varying intensities were shallower than in *Otof*$^{+/+}$ (black) SGNs. The sound intensity refers to the threshold of each SGN, defined by a spike rate increase of 20 Hz over spontaneous rate.

E Their dynamic range (the range of intensities over which the spike rate increased from 10% to 90% of the evoked rate) was normal.

F Spike rate increases in individual *Otof*$^{I515T/I515T}$ (red) SGNs in response to continuous presentation of amplitude-modulated sounds (CF, varying intensities, referenced to threshold like in D, modulation frequency 500 Hz) were much shallower than in *Otof*$^{+/+}$ (black) SGNs.

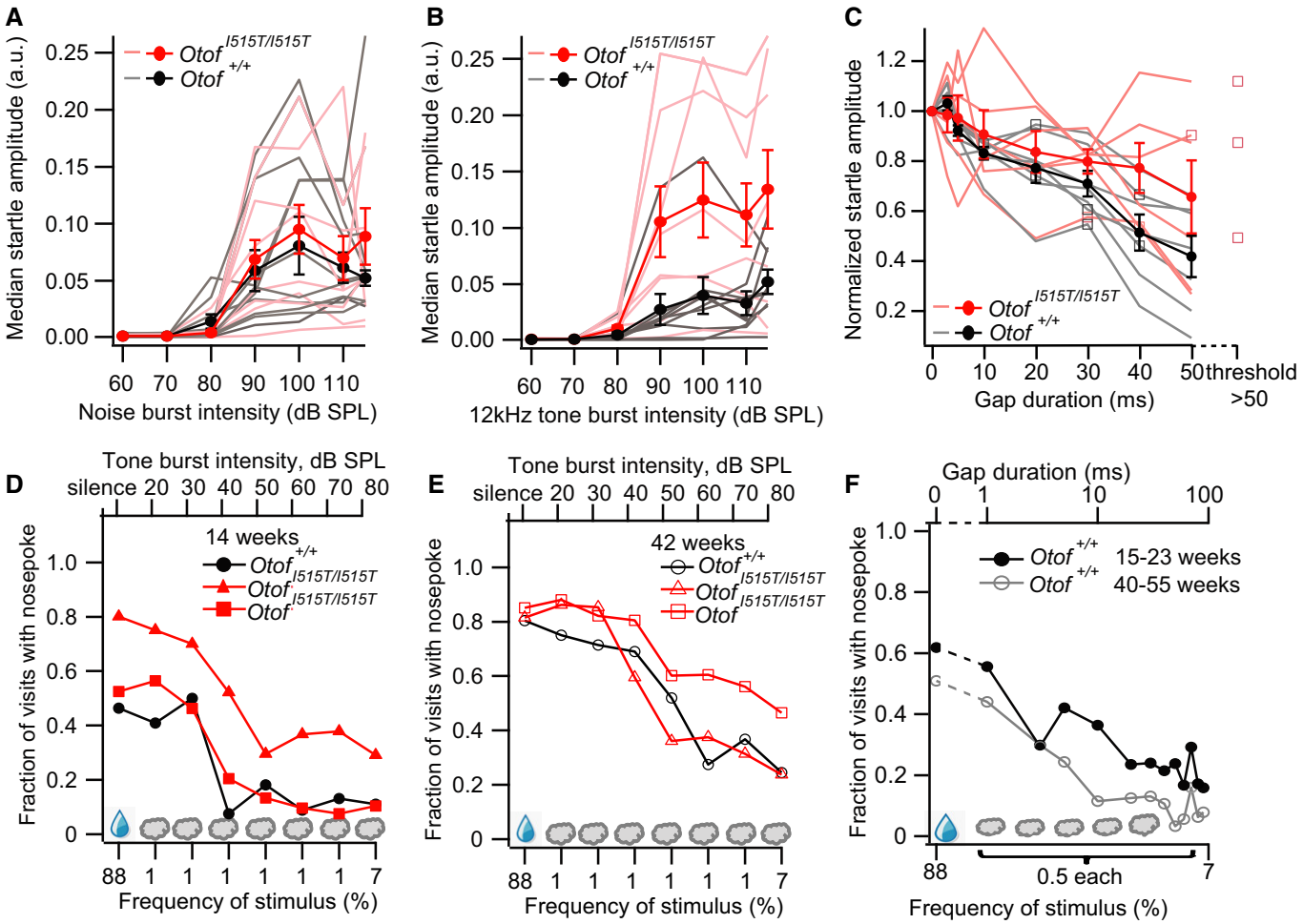

Figure EV3. Hearing impairment was assessed by startle responses and operant conditioning of mice.

A, B Acoustic startle responses to stimulation with 10 ms noise (A) or 12 kHz tone (B) bursts in *Otof*$^{I515T/I515T}$ (10 individuals pink, mean ± SEM red) and *Otof*$^{+/+}$ (9 individuals grey, mean ± SEM black) animals backcrossed to a CBA/J strain background.

C Prepulse inhibition of the startle response induced by silent gaps of varying duration was stronger in wild-type (eight individuals grey, mean ± SEM black) than in *Otof*$^{I515T/I515T}$ mice (eight individuals pink, mean ± SEM red). Gap detection thresholds were determined as the minimal duration of silent gaps in 70 dB background noise that were effective in significantly attenuating the amplitude of startle response elicited by 115 dB 12 kHz tone bursts (Mann–Whitney *U*-test followed by Bonferroni correction). Gap thresholds (squares) were elevated in *Otof*$^{I515T/I515T}$ mice (P = 0.04, Mann–Whitney *U*-test). In the control condition (no gap), the mean median startle amplitude for *Otof*$^{I515T/I515T}$ (0.07 ± 0.02) was identical to *Otof*$^{+/+}$ (0.07 ± 0.02; P = 0.99, *t*-test).

D Two *Otof*$^{I515T/I515T}$ mice (red) and one *Otof*$^{+/+}$mouse (black) learned to avoid drinking when they heard 12 kHz tone burst stimuli (400 ms, 3 Hz stimulus rate, 80 dB) during their visits to the soundproof corner of the "IntelliCage" operant conditioning system and drank water only when they did not perceive sounds. All three mice reacted to stimuli at 20 and 30 dB like for silence and for stimuli above 30 dB like for 80 dB, indicating comparable hearing thresholds near 35 dB for all three mice at the age of 14–21 weeks.

E Subjective hearing thresholds in the same mice from (D) increased by approximately 5–15 dB when the mice were retested at an age of 42–53 weeks.

F Behavioural gap detection did not show clear age-related changes in a wild-type mouse tested at 15–23 and 40–55 weeks.

A

```
human_e        163 PGEKSFR---------------RAGRSVFSAMKLGKNRSHKEEPQRPDEPAVLEMED 204
bos            163 SGEKSFR---------------RAGRSVFSAMKLGKNRPHKEEPQRQDEPAVLEMED 204
rat            163 PGEKSFR---------------RAGRSVFSAMKLGKTRSHKEEPQRQDEPAVLEMED 204
mouse var2     162 SGEKSFR---------------RAGRSVFSAMKLGKTRSHKEEPQRQDEPAVLEMED 203
mouse var4     162 SGEKSFR---------------RAGRSVFSAMKLGKTRSHKEEPQRQDEPAVLEMED 203
mouse var1     162 SGEKSFRSKGREKTKGGRDGEHKAGRSVFSAMKLGKTRSHKEEPQRQDEPAVLEMED 218
Xenopus        173 SGERAFK---------------RVGKGVFSAMKLGKTRPPKDESRKQDEPAVLETED 215
                       .**::*:              :.*:.*********.*  *:* :: ******* **
```

B

```
human_e       1234 PDRSAPSWNTTVRLLRRCRVLCNGGSSSHSTGEVVVTMEPEVPIKKLETMVKLD 1287
human_b        487 PDRSAPSWNT--------------------TGEVVVTMEPEVPIKKLETMVKLD  520
bos           1234 PDRSAPNWNTSGRLLQGRRGLYSGGPSSRLTGEVVVSMEPEVPIKKLETMVKLD 1287
rat           1234 PDRSAANWNTTVRLLRGYHMLCNGGPSSCPTGEVVVSMEPEVPVKKLETLVKLD 1287
mouse var2    1233 PDRSAPNWNTTVRLLRGCHRLRNGGPSSRPTGEVVVSMEPEEPVKKLETMVKLD 1286
mouse var4    1233 PDRSAPNWNT--------------------TGEVVVSMEPEEPVKKLETMVKLD 1266
mouse var1    1248 PDRSAPNWNT--------------------TGEVVVSMEPEEPVKKLETMVKLD 1281
Xenopus       1246 PDKNSQQWTTAAKLMNGYLAMTNGRPRSRTTGEIVINMEPEAPVKKMETMVKLE 1299
                   **:.: .*.*                    ***:*:.**** *:**:**:***:
```

C

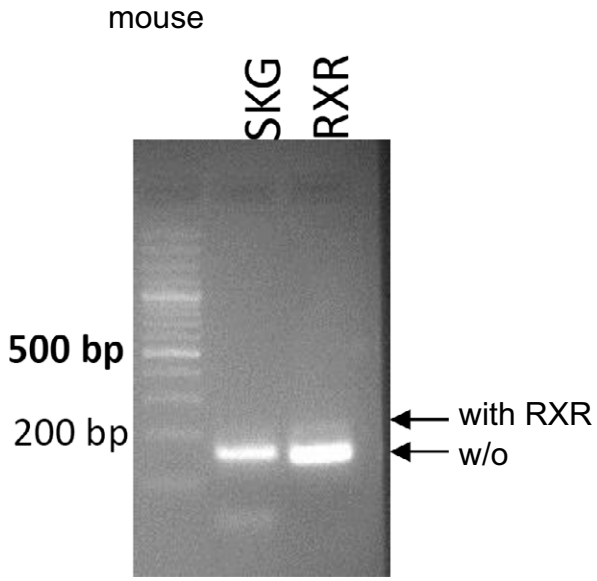

Figure EV4. Sequence variations in mouse and human otoferlin and comparison with other species.

A CLUSTAL Omega multiple sequence alignment for otoferlin homologues performed with the following sequences: Human otoferlin isoform e, NP_001274418.1; *Bos Taurus*, NP_001137579.1; *Rattus norvegicus*, NP_001263649; *Mus musculus* transcript variant 4, NM_001313767.1 (cDNA used in our experiments); *Mus musculus* transcript variant 1, NP_001093865.1; *Mus musculus* transcript variant 2, NP_114081.2; *Xenopus tropicalis*, XP_012826776.1. The presence of the 15 amino acid stretch SKG. . .GEH was tested in a PCR in (C).

B Sequence alignment, also including human otoferlin isoform b, NP_004793. Focus on the amino acid region between C_2D and C_2E bearing an arginine-rich sequence in human otoferlin isoform e, including an RXR motif (in red). Labelled in yellow is the human sequence that was introduced by site-directed mutagenesis into the mouse variant 4 for experiments in Fig 5.

C A PCR on mouse organ of Corti cDNA from P14 animals was performed to test for the expression of the mouse sequence variations. Left lane: using the primers AAGGACAGCCAGGAGACAGA and ATCTTGTCTTTGGGGCTCCT that bind before and after amino acid 168 in mouse variant 4 was used to distinguish between splice variants. For transcript variants 2 and 4, an amplicon of 155 bp was expected, whereas variant 1 should give rise to a 200-bp amplicon. The PCR indicates that almost exclusively the short variant is transcribed. Right lane: using primers TCATCTACCGACCTCCAGACC and CACATCCACCTTGACCACAGC binding before and after amino acid 1242 in mouse variant 4 expected to lead to an amplicon size of 148 bp for variants 1 and 4 or 208 bp for variant 2. The strong band at 148 bp indicates that the vast majority of cDNA molecules confirmed the expression of the short variant. In conclusion, our data indicate that transcript variant 4 seems to be the predominantly transcribed otoferlin isoform in mouse organs of Corti.